06 Apr 1995, 1:30 pm - 3:00 pm

Seismic Response of Embankment Dams

L. Caldeira
Laboratório Nacional de Engenharia Civil (LNEC), Lisboa, Portugal

P. Seco e Pinto
Laboratório Nacional de Engenharia Civil (LNEC), Lisboa, Portugal

J. Bilé Serra
Laboratório Nacional de Engenharia Civil (LNEC), Lisboa, Portugal

Proceedings: Third International Conference on Recent Advances in Geotechnical Earthquake Engineering and Soil Dynamics, April 2-7, 1995, Volume I, St. Louis, Missouri

Seismic Response of Embankment Dams

Paper No. 6.01

L. Caldeira, P. Seco e Pinto and J. Bilé Serra
Laboratório Nacional de Engenharia Civil (LNEC), Lisboa, Portugal

SYNOPSIS: This study is intended as a contribution towards a better understanding of the seismic response of embankment dams. Laboratory tests for the determination of static and dynamic mechanical properties of the material are described. A parametric study is performed varying the main source of earthquakes, the height of the dam, the type of the materials and the core position (central and upstream sloping core). The dynamic analyses have made possible the identification of hazard scenarios and particularly the evaluation of stability and residual deformation of the dams.

INTRODUCTION

The purpose of the present study is to improve the state of knowledge on the key factors of the seismic behaviour of embankment dams. In order to achieve a comprehensive as well as enlarged picture of the subject, three zoned earth dams are analyzed: Borde Seco Dam, Las Cuevas Dam and Alvito Dam. The dams properties such as geometry and constitutive materials and the corresponding seismic environment were selected to get a broad and representative picture of the subject.

Borde Seco Dam, located in Venezuela, is a 122 m high dam with a thick central core. Upstream and downstream shells, a filter, a drain and a protection zone of the upstream shell consist essentially of granular materials (Figure 1).

Las Cuevas Dam, located in Venezuela, is a 92 m high dam, with a thin upstream sloping clay core and shells and a draining zone of granular materials (Figure 2).

Alvito Dam, constructed in Portugal, is a 40 m high dam with a cohesive central core, and shells of decomposed schist materials (Figure 3).

The static and dynamic geotechnical characterization of the main materials were based in triaxial monotonic compression tests, simple shear cyclic tests and cross-hole tests.

Due to some limitations of the simple shear device (Sêco e Pinto, 1990), as far as more elaborated modelling is concerned, and to the extent of the present study, the linear equivalent model was used in a finite element analysis of plane strain equilibrium (Bilé Serra, 1991). The stresses prior to the earthquake analysis were calculated using the hyperbolic model.

A detailed comparison of the dams behaviour under a post-reservoir filling earthquake is performed and the conclusions related with the key factors of the seismic behaviour are drawn. Limitations of space do not allow to show all the results, which are presented in Caldeira (1994).

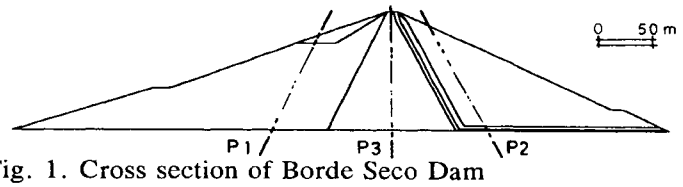

Fig. 1. Cross section of Borde Seco Dam

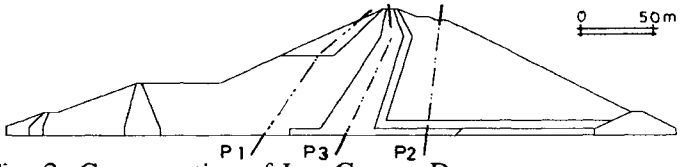

Fig. 2. Cross section of Las Cuevas Dam

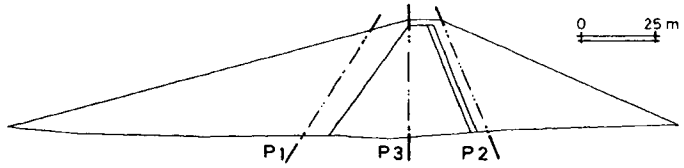

Fig. 3. Cross section of Alvito Dam

STATIC ANALYSES

The static analyses after the first reservoir filling were carried out using the hyperbolic model. The hyperbolic parameters were determined from undrained unconsolidated triaxial compression tests.

Table 1 shows the maximum horizontal, vertical and total cumulated displacements, as well as the maximum vertical stresses at the end of the construction and after the first filling of the reservoir of the studied dams.

Due to the soil nature (only granular materials are incorporated) Borde Seco Dam has smaller deformability. The maximum vertical stresses are directly related to the height of the dams.

Table 1. Maximum static displacements and vertical stresses of Borde Seco Dam, Las Cuevas Dam and Alvito Dam

		Borde Seco Dam	Las Cuevas Dam	Alvito Dam
Construction phase	Maximum horizontal displacement (m)	0.183	0.267	0.132
	Maximum vertical displacement (m)	0.262	0.418	0.640
	Maximum total displacement (m)	0.286	0.418	0.640
	Maximum vertical stress (kPa)	2000	1589	950
After reservoir filling	Maximum horizontal displacement (m)	0.256	0.372	0.158
	Maximum vertical displacement (m)	0.269	0.415	0.621
	Maximum total displacement (m)	0.347	0.451	0.623
	Maximum vertical stress (kPa)	2390	1600	940

At Las Cuevas Dam and Alvito Dam, the vertical stress isolines show a stress transfer from the clay core to the shell materials (Figures 5 and 6). This arching effect is very slight in Borde Seco Dam that exhibits a behaviour of an homogeneous dam (Figure 4).

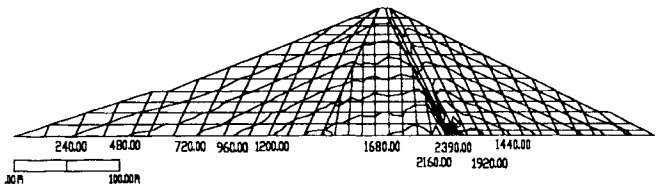

Fig. 4. Vertical stress isolines (kPa) after the first reservoir filling at Borde Seco Dam

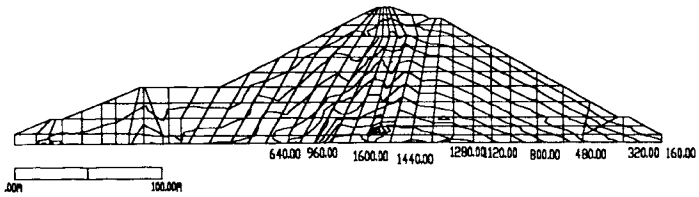

Fig. 5. Vertical stress isolines (kPa) after the first reservoir filling at Las Cuevas Dam

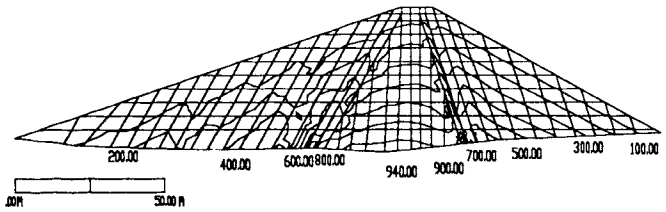

Fig. 6. Vertical stress isolines (kPa) after the first reservoir filling at Alvito Dam

DYNAMIC ANALYSES

Seismic input

The horizontal seismic input is defined by three synthetic accelerograms generated for nearby sources and faraway sources. These accelerograms were used also in the vertical direction after being scaled by a convenient correction factor. Combining independent accerelograms in both horizontal and vertical directions a total of six pairs for each type of seismic action were obtained.

As the dams are located in different seismic areas, the associated seismic risk is also different. Therefore, the generation of accelerograms is based in different data and parameters, according to the seismic risk studies made for the purpose.

For Borde Seco Dam and for Las Cuevas Dam, a life time of 100 years and exceedance probability of 10% were considered. For each seismic input type (nearby and faraway sources) the maximum horizontal movements at bedrock were estimated and the duration is computed by the Trifunac and Brady (1975) relation. The elastic response spectra are determined using the Newmark and Hall (1982) equations and the power spectral density functions were computed. Compatible horizontal acceleration time histories were obtained by superposition of harmonic components. Finally, the Jennings et al (1968) intensity function allows one to model the acceleration time histories in order to obtain pseudo non stationary accelerograms.

For Alvito Dam, the Portuguese Safety Code (RSA (1983)) was followed. This code presents power spectral density functions of the horizontal acceleration and seismic durations as a function of the structural site and the seismic action type. According to RSA, the seismic inputs are gaussian stochastic stationary processes. The correspondent accelerograms are also generated by superposition of harmonic components.

Table 2 synthetizes the peak values of bedrock horizontal acceleration, the duration of accelorograms and the corrective factor used to scale the vertical component of acceleration from the horizontal one for each dam and each seismic action type.

Table 2.Main accelerogram characteristics of Borde Seco , Las Cuevas and Alvito Dams

	Borde Seco Dam		Las Cuevas Dam		Alvito Dam	
	Nearby action	Faraway action	Nearby action	Faraway action	Nearby action	Faraway action
Bedrock maximum horizontal acceleration (m/s²)	4.2	2.3	4.61	2.94	2.2	1.1
Duration (sec)	35	55	20	55	10	30
Vertical acceleration / horizontal acceleration	0.75	0.75	0.75	0.75	0.66	0.66

Dynamic soil properties

The dynamic soil properties needed for the application of the linear equivalent model are: maximum shear modulus (G_{max}),

variation of ratio between the current shear modulus (G) and the maximum shear modulus (G_{max}) with the shear strain (γ) and variation of the damping ratio (D) with the shear strain.

For evaluating the dynamic soil properties constant volume cyclic simple shear tests (with a NGI equipment) were conducted. The vertical stress and the amplitude of the shear stress was varied from test to test. The cyclic evolution of the shear strain and of the pore pressure (assumed opposite to the vertical stress variation) was recorded. From the hysteretic loops of shear stress versus shear strain, the shear modulus and the damping ratio were computed for different shear strain levels. Unfortunately, the shear strain range obtained with NGI type equipments is limited and the strain range likely to occur during the seismic analysis is not fully covered, namely G_{max} can not be determined.

The extrapolation of the test results for different shear strain levels was based on empirical relations established for G_{max} (Goto et al (1987)), on cross-hole tests results available for similar materials, on empirical curves of $G/G_{max}(\gamma)$ and of $D(\gamma)$ obtained by others researchers (Sun et al (1988)). For each soil, a comparison between the simple shear cyclic test results and the available empirical curves was made and the best estimated G_{max} value and curves were adopted. For G_{max} the following general equation was followed:

$$G_{max} = A \cdot F(e) \cdot (\sigma'_m)^n \cdot p_a^{1-n} \qquad (1)$$

where σ'_m represents the effective mean principal stress, p_a is the atmospheric pressure, F(e) is a void ratio function and A and n are soil parameters. The adopted curves G/G_{max} and D versus γ are illustrated in Figure 7.

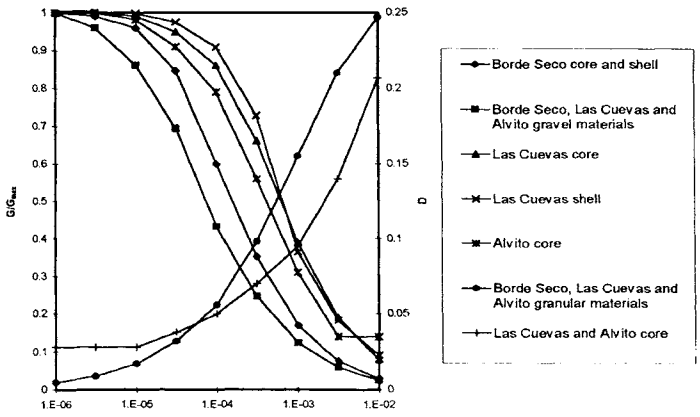

Fig. 7. Dynamic soil properties

Dominant frequencies

The dominant frequencies that were achieved for the most participant modes are shown in Table 3. Those were obtained after iterating the soil properties so as to achieve the compatibility between computed shear strains and shear modulus and damping ratio values.

The dominant frequencies are related with the height of the studied dams, being minimum at Borde Seco and maximum at Alvito.

Table 3. Dominant frequencies of the first two most participative modes of Borde Seco Dam, Las Cuevas Dam and Alvito Dam

Most participative modes	Borde Seco Dam				Las Cuevas Dam				Alvito Dam			
	Nearby action		Faraway action		Nearby action		Faraway action		Nearby action		Faraway action	
	Mode no.	Freq. (Hz)	Mode no.	Freq. (Hz)	Mode no.	Freq. (Hz)	Mode no.	Freq. (Hz)	Mode no.	Freq. (Hz)	Mode no.	Freq. (Hz)
First	1	0.29	1	0.39	1	0.71	1	0.73	1	1.18	1	1.19
Second	3	0.54	3	0.70	2	1.05	2	1.03	3	1.92	3	2.04

Accelerations

The maximum horizontal (a_h^{max}) and vertical (a_v^{max}) accelerations at the base, at the contour, and in three profiles crossing the upstream shell (profile P1), the downstream shell (profile P2) and the core (profile P3) of each dam are presented in Table 4.

In general, the maximum accelerations of upstream shell are lower than those observed in other profiles, as a consequence of lower initial stresses due to the water effect. The maximum accelerations took place at Las Cuevas Dam, due to the major stiffness associated to the larger seismic intensity. Comparing the base acceleration with the crest acceleration, it may be concluded that the amplification factor is maximum at Las Cuevas Dam and Alvito Dam for the faraway earthquake.

Table 4. Maximum horizontal and vertical accelerations of Borde Seco Dam, Las Cuevas Dam and Alvito Dam

Localization	Seismic action	Borde Seco Dam		Las Cuevas Dam		Alvito Dam	
		a_h^{max} (m/s²)	a_v^{max} (m/s²)	a_h^{max} (m/s²)	a_v^{max} (m/s²)	a_h^{max} (m/s²)	a_v^{max} (m/s²)
Profile P1	nearby	2.9	3.1	5.1	5.5	2.8	1.7
	faraway	2.0	1.8	7.2	4.6	2.5	1.5
Profile P2	nearby	3.5	3.2	6.8	6.3	3.4	3.0
	faraway	2.4	1.9	5.2	4.8	2.8	1.6
Profile P3	nearby	5.0	3.1	6.4	3.7	3.6	1.7
	faraway	3.8	1.8	9.1	5.1	3.0	1.2
Contour	nearby	5.0	4.1	8.8	5.2	3.9	2.8
	faraway	4.2	2.6	9.1	3.7	3.3	2.0
Base	nearby	4.2	3.15	4.61	3.46	2.2	1.45
	faraway	2.3	1.73	2.94	2.21	1.1	0.73

Seismic shear stresses

The maximum seismic shear stresses evolution along the P1, P2 and P3 profiles for all combinations of each seismic action type are described in Tables 5, 6 and 7, respectively.

The following trends may be observed: (i) for increasing height of the dam the peak shear stress value decreases; (ii) for the same height the seismic shear stresses are larger in the stiffer materials; and (iii) the faraway earthquake produces maximum shear stress values lower than the correspondent values due to the nearby earthquake.

Table 5. Maximum shear stresses (kPa) in profile P1 produced by earthquake 1 in Borde Seco Dam, Las Cuevas and Alvito Dam

Borde Seco Dam		Las Cuevas Dam		Alvito Dam	
Nearby action	Faraway action	Nearby action	Faraway action	Nearby action	Farway action
147	114	176	156	41	44
119	94	100	115	40	46
105	83	91	102	36	41
88	68	72	77	27	29
76	62	56	52	12	9
-	-	32	27	-	-

Table 6. Maximum shear stresses (kPa) in profile P2 produced by earthquake 1 in Borde Seco Dam, Las Cuevas Dam and Alvito Dam

Borde Seco Dam		Las Cuevas Dam		Alvito Dam	
Nearby action	Faraway action	Nearby action	Faraway action	Nearby action	Faraway action
151	102	176	156	48	51
145	115	161	147	44	50
137	96	145	143	37	47
125	72	103	111	35	37
80	70	65	60	27	22
29	27	-	-	7	6

Table 7. Maximum shear stresses (kPa) in profile P3 produced by earthquake 1 in Borde Seco Dam, Las Cuevas Dam and Alvito Dam

Borde Seco Dam		Las Cuevas Dam		Alvito Dam	
Nearby action	Faraway action	Nearby action	Faraway action	Nearby action	Faraway action
168	120	214	193	99	74
139	103	155	160	92	89
129	89	133	136	63	82
121	83	120	120	56	63
91	79	90	82	36	32
49	43	29	30	7	5

Equivalent number of uniform cycles

The equivalent number of uniform cycles of all finite elements of each dam was computed from the shear stress time histories by using Seed et al (1975) approach. A summary of the maximum (N_{max}) and minimum (N_{min}) values calculated at three horizontal sections, whose vertical position is shown, is displayed at Table 8.

Alvito Dam shows a higher value because of the stationary nature of the prescribed seismic action. The faraway earthquake generates a larger number cycles than the nearby one, since it lasts longer. Comparing the behaviour of Borde Seco and Las Cuevas Dam one may conclude that, due to the greater energy dissipation and lower stiffness of its materials Borde Seco Dam shows a lower value of equivalent uniform cycles.

Table 8. Maximum and minimum number of uniform equivalent cycles of Borde Seco Dam, Las Cuevas Dam and Alvito Dam

Borde Seco Dam					Las Cuevas Dam					Alvito Dam				
Height	Nearby action		Faraway action		Height	Nearby action		Faraway action		Height	Nearby action		Farway action	
(m)	N_{min}	N_{max}	N_{min}	N_{max}	(m)	N_{min}	N_{max}	N_{min}	N_{max}	(m)	N_{min}	N_{max}	N_{min}	N_{max}
246.3	2	8	4	12	637.7	3	10	4	16	179.5	4	15	4	26
281.1	3	8	3	12	666.5	3	8	5	15	191.5	4	14	6	31
315.2	3	7	5	10	694.5	3	13	4	16	200.5	6	16	10	28

SEISMIC BEHAVIOUR ANALYSIS

According to Seed et al (1975) methodology, the dam stability evaluation is based in the comparison between the shear stresses results, determined in the dynamic analysis, and the shear stresses obtained in simple shear tests, capable to produce in a specimen a prescribed level of strain in a specified number of uniform cycles. So, the dam seismic behaviour must be evaluated not only by the dynamic analysis results but also by considering the cyclic strength of the material (Sêco e Pinto, 1993).

Cyclic material strength

Based in cyclic simple shear test results, equations relating the cyclic shear stress with the vertical stress (σ'_v), and with the strain level, for a selected number of uniform cycles, were interpolated. The pore pressure ratio (i.e. the current pore pressure divided by the initial vertical stress) showed to be a function of the shear strain level only.

Tables 9 and 10 present maximum (determined with maximum vertical stress of each dam, valid at the dam base) and minimum (determined with zero vertical stress, valid at the crest) laboratory cyclic shear stress amplitudes and pore pressure ratios developed in 12 uniform cycles capable to induce 1, 2, 5 and 10% of shear strain. These were obtained in the most representative geotechnical materials in the dams.

Table 9. Laboratory cyclic shear stress amplitudes (kPa) capable to induce strain levels of 1, 2, 5 and 10% in Borde Seco Dam, Las Cuevas Dam and Alvito Dam materials

γ (%)	Borde Seco Dam						Las Cuevas Dam				Alvito Dam			
	Core material		Upstream shell material		Downstream shell material		Core material		Shell material		Core material		Shell material	
	Crest	Base	Crest	Base	Crest	Base	Crest	Base	Crest	Base	Crest	Base	Crest	Base
1	15	187	11	196	9	256	22	175	15	141	15	132	16	106
2	18	220	13	231	12	305	30	209	17	166	18	154	18	130
5	21	264	16	278	14	371	40	255	20	200	21	184	21	160
10	24	297	18	313	17	421	48	290	22	225	24	206	23	184

Table 10. Laboratory pore pressure ratios (%) for shear strain levels of 1, 2, 5 and 10% in Borde Seco Dam, Las Cuevas Dam and Alvito Dam materials

γ (%)	Borde Seco Dam			Las Cuevas Dam		Alvito Dam	
	Core material	Upstream material	Downstream material	Core material	Shell material	Core material	Shell material
1	46.5	46.2	41.9	34.5	55.9	31.4	37.3
2	59.6	60.1	57.4	45.5	68.5	46.6	50.2
5	77.1	78.5	78.0	60.0	85.3	66.8	67.2
10	90.3	92.4	93.5	71.0	98.0	82.0	80.0

The cyclic shear stresses are maximum at Borde Seco Dam and minimum at Alvito Dam for the same shear strain level and for the maximum vertical stress. The pore pressure ratios are smaller in the cohesive type materials (Las Cuevas core and Alvito materials).

Stability evaluation

The initial liquefaction state may be achieved locally or globally causing excessive deformations to occur and the soil to weaken. The deformation values may be estimated by considering the potential strain values. Those are obtained in laboratory tests performed under a constant cyclic stress equal to 65% of the maximum seismic shear stress, after a convenient number of uniform cycles has been applied.

The pore pressure level is evaluated by associating a pore pressure ratio to each of the finite elements. Initial liquefaction occurs when the pore pressure ratio is equal to unity. All the materials in study were used in a dense state. Therefore, the expected deformations should be small and the probability of liquefaction occurrence is null. Nevertheless, the initial liquefaction condition is useful to predict a deterioration of the materials strength, within a situation of limited deformations occurrence.

The deformation analysis is based in the potential strain calculations. Potential strains less than 5% do not endanger the seismic stability of the dams. Potential strains between 5 and 10% are considered to be moderate and it is necessary to have its spatial distribution to estimate the dam potential risk. Potential strains greater than 10% are considered to be intense.

Tables 11 and 12 describe the maximum (dp_{max}) and average (dp_{av}) potential deformations and the maximum pore pressure ratios (R_u max) computed in each representative material and in the overall dam, respectively. The cyclic simple shear tests preclude meaningful results for shear strains greater than 10%. So, if the cyclic shear stresses from the dynamic analysis surpass the laboratory shear stresses corresponding to a shear strain of 10%, only the indication of ">10" is placed.

Figures 8, 9 and 10 show the potential deformation distribution along Borde Seco Dam, Las Cuevas Dam and Alvito Dam.

Table 11. Potential deformations of Borde Seco Dam, Las Cuevas Dam and Alvito Dam

Localization	Borde Seco Dam				Las Cuevas Dam		Alvito Dam			
	Nearby action		Faraway action		Nearby action	Faraway action	Nearby action		Faraway action	
	dp_{max} (%)	dp_{av} (%)	dp_{max} (%)	dp_{av} (%)	dp_{max} (%)	dp_{max} (%)	dp_{max} (%)	dp_{av} (%)	dp_{max} (%)	dp_{av} (%)
Upstream shell	5.3	2.00	2.2	0.78	>10	>10	0.6	0.23	0.8	0.28
Core	3.8	0.8	1.4	0.40	3.5	3.9	1.3	0.63	3.1	0.52
Downstream shell	6.8	1.05	2.6	0.54	>10	>10	0.3	0.21	0.4	0.24
Overall	6.8	1.45	2.6	0.63	-	-	1.3	0.25	3.1	0.32

Table 12. Maximum pore pressure ratios of Borde Seco Dam, Las Cuevas Dam and Alvito Dam

Localization	Borde Seco Dam		Las Cuevas Dam		Alvito Dam	
	Nearby action	Faraway action	Nearby action	Faraway action	Nearby action	Farway action
	R_u max (%)	R_u max(%)	R_u max(%)	R_u max(%)	R_u max (%)	R_u max (%)
Upstream shell	80	62	-	-	27	34
Core	72	53	54	56	36	56
Downstream shell	85	64	-	-	17	19

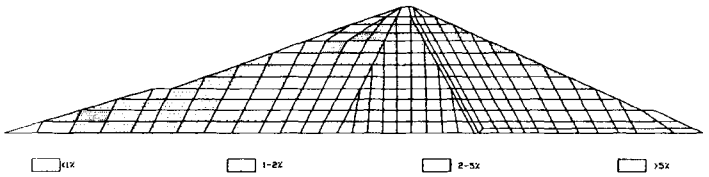

Fig 8a. Potential deformation distribution along Borde Seco Dam (nearby action)

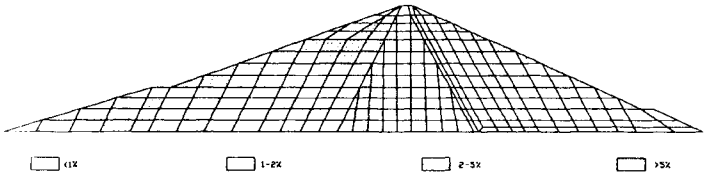

Fig 8b. Potential deformation distribution along Borde Seco Dam (faraway action)

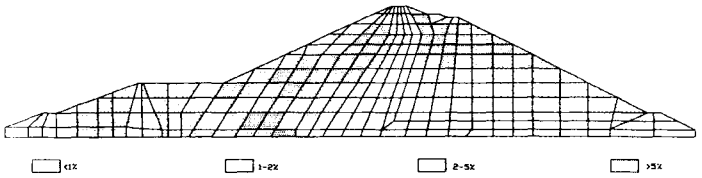

Fig 9a. Potential deformation distribution along Las Cuevas Dam (nearby action)

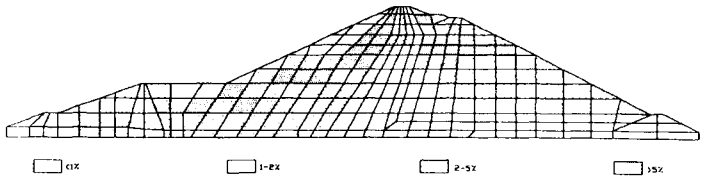

Fig 9b. Potential deformation distribution along Las Cuevas Dam (faraway action)

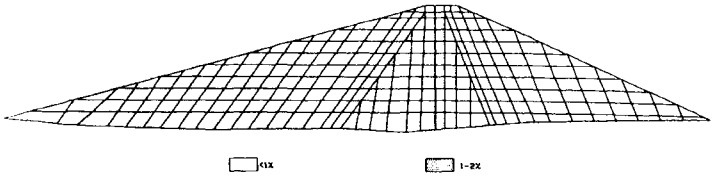

Fig 10a. Potential deformation distribution along Alvito Dam (nearby action)

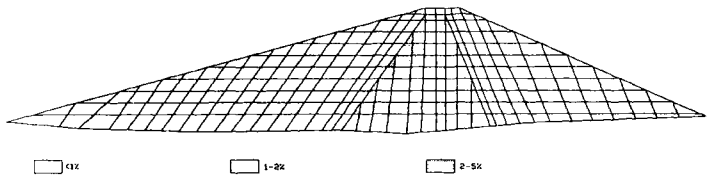

Fig 10b. Potential deformation distribution along Alvito Dam (faraway action)

CONCLUSIONS

The present study was intended to contribute towards a better understanding of the seismic response of embankment dams.

The following conclusions can be pointed out:

1) The dominant frequencies are related with the height of the dam, with minimum values at Borde Seco Dam and maximum values at Alvito Dam.

2) The maximum accelerations were calculated at Las Cuevas Dam and are associated with the larger seismic intensity.

3) The shear stresses present the following path: (i) decrease with the increasing of the height of the dam; (ii) for the same height of the dam the shear stresses increase with the stiffness of the materials; (iii) the maximum shear stresses are lower for the faraway earthquakes in comparison with the nearby earthquakes.

4) The equivalent number of uniform cycles shows the following trends: (i) it increases for the faraway earthquakes in comparison with the nearby earthquakes as a consequence of its higher durations; (ii) it increases with the duration of the stationary range of the acceleration time histories.

5) The seismic action plays an important role on the seismic behaviour of the dams. For similar heights one may conclude that the type of the materials and the core position have a second order importance.

ACKNOWLEDGMENTS

The work reported herein is a part of a long-range research programme "Dynamic Analysis of Embankment Dams" carried out at the Laboratório Nacional de Engenharia Civil (LNEC). Permission to publish this paper has kindly been given by the Director.

REFERENCES

Bilé Serra, J. P., "Seismic Analysis of Geotechnical Structures by Stochastic Process Theory", 5th International Conference on Soil Dynamics and Earthquake Engineering, 1991.

Caldeira, L., "Dynamic Behaviour of Embankment Dams - Evaluation Methods" (in portuguese), PhD thesis, LNEC, 1994.

Goto, S., Syamoto, Y. and Tamaoki, K., "Dynamic Properties of Undisturbed Gravel Samples Obtained by the In-Situ Freezing Method", 8th Asian Regional Conference on Soil Mechanics and Foundation Engineering, Kyoto, 1987, pp. 223-236.

Jennings, P. C., Housner, G. W. and Tsai, N. C., "Simulated Earthquake Motions", Earthquake Engineering Research Laboratory Report, California Institute of Technology, 1968.

Newmark, N. and Hall, W. S., "Earthquake Spectra and Design", EERI Monograph Series, Berkeley, 1982.

RSA , "Regulamento de Segurança para Estruturas de Edifícios e Pontes", 1983.

Sêco e Pinto, P. S., "Dynamic Characterization of Soils. Natural Hazards and Engineering Geology - Prevention and Control of Landslides and other Mass Movements", European School of Climatology and Natural Hazard Course, 1990, pp. 53-68.

Sêco e Pinto, P. S., "Dynamic Analysis of Embankment Dams", Proceedings of the Seminar on Soil Dynamics and Geotechnical Earthquake Engineering, Editor Sêco e Pinto, P. S., 1993, A. A. Balkema, pp. 159-269.

Seed, H. B., Idriss, I. M., Makdisi, F. and Benerjee, N., " Representation of Irregular Stress Time Histories by Equivalent Uniform Stress Series in Liquefaction Analyses", Report No. UCB/EERC 75-29, 1975.

Sun, J., Golesorkhi, R. and Seed, H., "Dynamic Moduli and Damping Ratios for Cohesive Soils", Report No. UCB/EERC-88/15, 1988.

Trifunac, M. D. and Brady, A. G., "Corrections of Peak Acceleration, Velocity and Displacement with Earthquake Magnitude, Distance and Site Conditions", Earthquake Engineering and Structure Dynamics, Vol. 4, 1975, pp. 455-471.